1. Introduction

In recent decades, the cold-formed steel (CFS) sections are increasingly used in a low to medium rise buildings as primary elements, even in seismic prone regions. In which, the shear wall panel (SWP) is the main lateral load resisting system; it is made of CFS C-shaped framing members (studs and tracks) attached to steel or wood sheathing using screw connections. The strength and energy dissipation capacity of the SWP depend essentially on the inelastic behaviour of its framing-to-sheathing connections. Under repeated cyclic deformation, the formed hysteresis loops are characterised by severe strength and stiffness deteriorations as well as a pinching effect. These phenomenons which affect most the post-elastic behaviour must be taken into account in the dynamic nonlinear analyses. The basic requirement to perform such an analysis is the availability of an accurate constitutive model capable of simulating the SWP response when subjected to a quasi-static or dynamic lateral loading. In this document, smooth hysteresis models for wood and steel sheathed CFS SWP based on the hysteresis model developed by Lowes LN and Altoontash A (2003) that take into account strength and stiffness degradation with pinching effect have been developed. The main advantage of these models is that all their parameters are directly related to the physical and mechanical characteristics of the SWP. The models have been implemented in OpenSees program, as user-defined uniaxial materials using dynamic link libraries (DLLs). The accuracy of the proposed models is validated using several experimental test results obtained from literature. The benefit of implementing the models in OpenSees is that it will help to perform different types of analysis of cold formed steel structures for both research and design purposes.

2. Hysteresis model

Smooth hysteresis models for wood and steel sheathed CFS SWP based on the model proposed by Lowes LN and Altoontash A (2003) that take into account strength and stiffness degradation with pinching effect have been developed. The uniaxial hysteresis models of wood and steel sheathed CFS SWP consist of three parts: backbone curves of the hysteresis loops (states 1 and 2), hysteresis criteria (unloading-reloading path: states 3 and 4) and degradation criteria (Fig.1). The following sections will respectively introduce the expressions of the three parts.

These models can represent characteristics observed in experiments such as the response at time/instance that depends not only on the instantaneous displacement, but also on its past history, such as the input and response at earlier times.

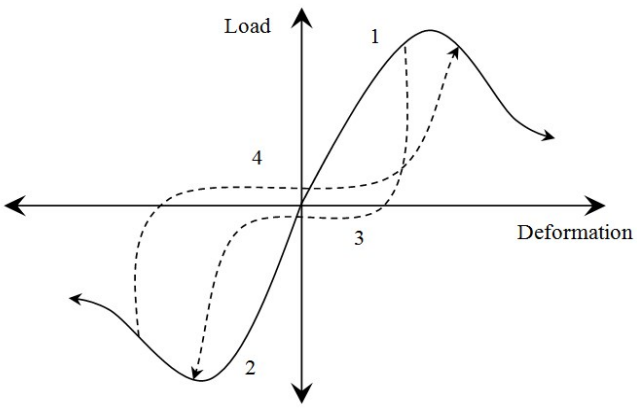

Fig.1: Uniaxial hysteresis model states.

2.1 Backbone curve

Maximum Lateral shear strength and the associated displacement are assessed using two analytical methods for wood sheathed and steel sheathed CFS SWP proposed by, respectively, Xu L and Martinez J (2007), and Yanari N and Yu C (2014) which take into account a wide range of factors that affect the behaviour and strength of a CFS SWP, namely: material properties, thickness and geometry of sheathing and framing, spacing of studs, construction details such as size and spacing of sheathing-to-framing connections.

Equivalent energy elastic-plastic (EEEP) multi-linear model, as shown in Fig.2, is used to determine the key points' coordinates through which the envelop curve passes. This model assumes an envelope curve that is capable of dissipating an equivalent amount of energy as the real shear wall does (area A_1=A_2).

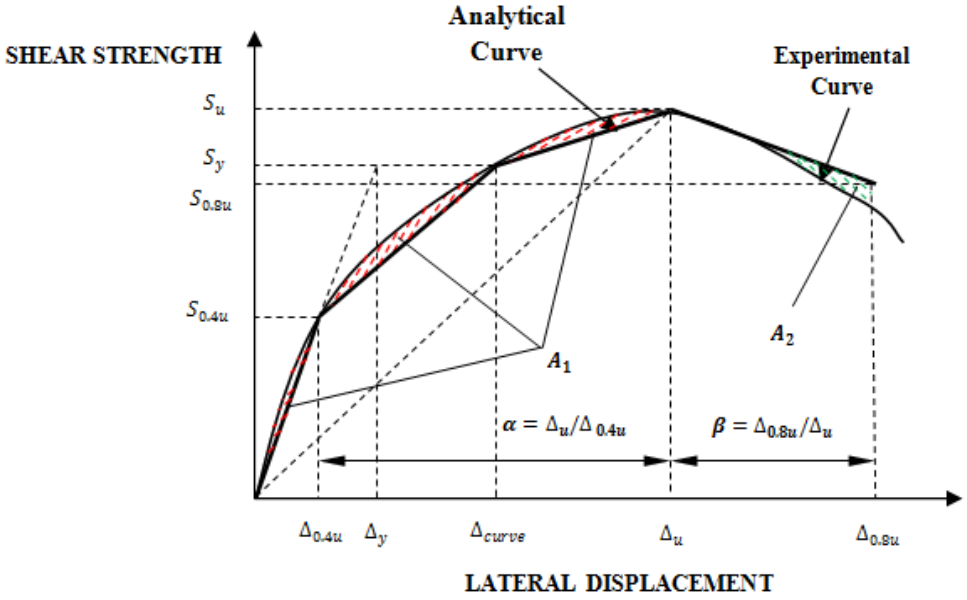

Fig.2: Multi-linear envelope curve.

where

- S_u : Ultimate shear strength;
- Δ_u : Displacement corresponding to S_u;
- $S_{0.4\,u}$: Strength corresponding to 40% of the ultimate strength value;
- $\Delta_{0.4\,u}$: Displacement corresponding to $S_{0.4u}$;
- $S_{0.8\,u}$: Strength corresponding to 80% of the ultimate strength value;
- $\Delta_{0.8\,u}$: Displacement corresponding to $S_{0.8u}$;
- S_y : Yield strength limit idealized as 85% of the ultimate strength value;
- Δ_y : Displacement corresponding to S_y;
- $k_e = \frac{S_{0.4\,u}}{\Delta_{0.4\,u}}$: Elastic stiffness;
- Δ_{curve} : Displacement adjusted so that the area (A_{multi}) limited by the x-axis and the multi-linear curve till the failure point is equal to that limited by the experimental curve.

$$\Delta_{curve} = \frac{S_y.(\Delta_u+\Delta_y-2.\Delta_{0.8\,u}-\Delta_{0.4\,u})+S_u.\Delta_{0.8\,u}+S_{0.8\,u}.(\Delta_{0.8\,u}-\Delta_u)}{0.6.S_u} \quad (1)$$

According to the experimental results of tests conducted by Serrette et al. (2009) on shear wall panels with wood sheathing attached by pins, where the displacement ratio α of the ultimate displacement Δ_u to the elastic displacement $\Delta_{0.4u}$ value varies from 8.61 to 10.29, with an average value of 9.25. The ratio β of the failure displacement limit $\Delta_{0.8u}$ to ultimate displacement Δ_u varies from 1.0 to 1.63 with an average value of 1.40. Given the similarity between pins and screws nonlinear behaviour, for the simplicity, the authors applied the abovementioned factors in CFS SWP with screw connections.

Given the key points shown in Fig.2, a curved envelope is adjusted by applying the B-Spline algorithm; this achieves the curvature for the states 1 and 2 of the hysteresis model. As can be seen in Fig.3, a good agreement between the envelope curves of a SWP developed analytically and the one derived from experimental monotonic tests (Branston et al. (2006) and Balh (2010)).

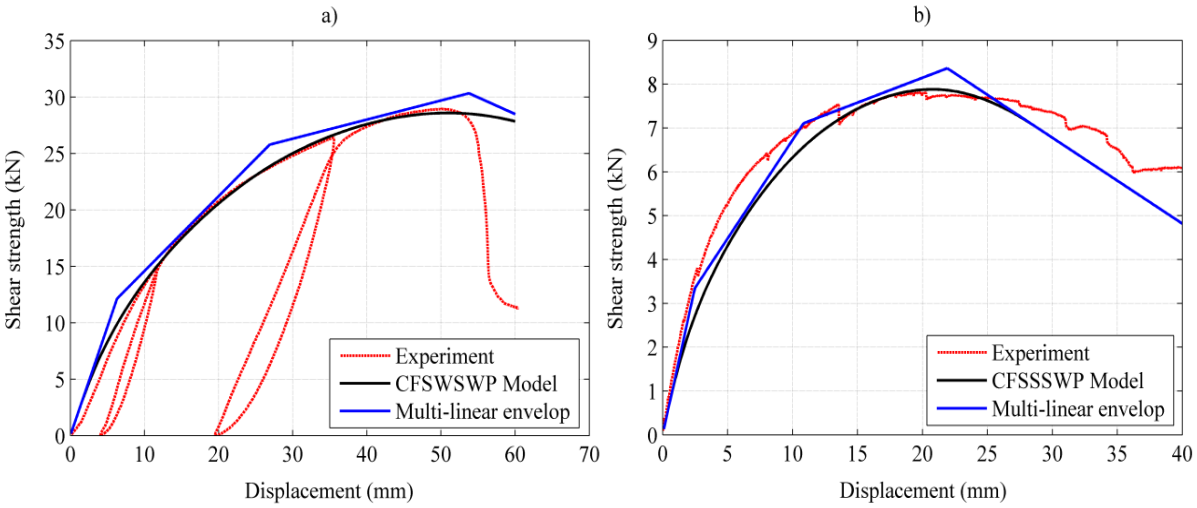

Fig. 3. Comparison between analytical and experimental monotonic curves.

2.2 Hysteresis criteria

In addition to the envelope curve, the proposed hysteresis model requires the introduction of parameters that define the strength and stiffness degradation, as well as the pinching effect under cyclic loading. On the basis of information deduced from the CFS SWP experimental database, empirical relationships to assess the degradation parameters are proposed hereafter.

The experimental tests results show a pinched shear strength-lateral displacement history. Pinching caused by the loss of stiffness at the connection level, where a gap or slot is formed around the screw head when the sheathing is damaged; this phenomenon is represented using the uniaxial material model with parameters defined as follow:

- Unloading stiffness: assumed equal to the elastic stiffness;
- Shear displacements at which reloading occurs: defined to be 0.448 of maximum historic shear displacement in both positive and negative directions;
- Shear strengths at which reloading occurs: defined to be 0.183 and 0.244 of maximum historic shear displacement, respectively, in positive and negative direction;

• The ratio of strength developed upon unloading from negative and positive loads to, respectively, the maximum and minimum strengths developed under monotonic loading: defined to be -0.08.

The curvature for the states 3 and 4 is obtained with the monotone cubic spline algorithm as the generated curve always passes through the 4 points in phases 3 and 4 while ensuring the monotony of the curve. When applying the monotone cubic spline a fifth point is taken into account in order to improve the derivability of the curve when it is attached to the envelope curve (states 1 and 2), this fifth point is added after the last point of the state with a chosen offset of (20,1) in the positive quadrant and (-20,-1) in the negative quadrant.

The above-defined unloading-reloading paths are shown in Fig.4.

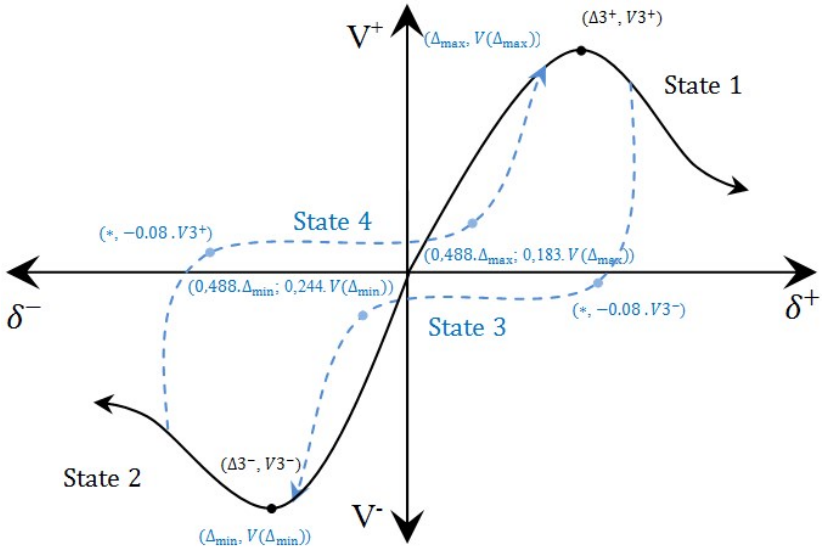

Fig.4: Unloading-reloading paths of the proposed hysteresis model.

2.3 Degradation criteria

Compared to the monotonic test result, the hysteresis response of CFS SWP exhibits strength deterioration (Fig.5 a); even if the displacement associated to peak strength has not been reached. This deterioration is attributed to the formation of play around the screw head during the first excursion in a given direction which results in a lower strength capacity, simply because we can expect less resistance from crushed wood around the fastener. As for as the steel sheathed SWP is concerned, this difference in strength capacity was not noticed due to the fact that the failure mode of such a type of wall is initiated by the elastic buckling of steel sheet. Hence, the cyclic nature of loading enables the SWP to regain its shape which allows the latter to generate the same strength as when if it were loaded monotonically (Fig.5 b).

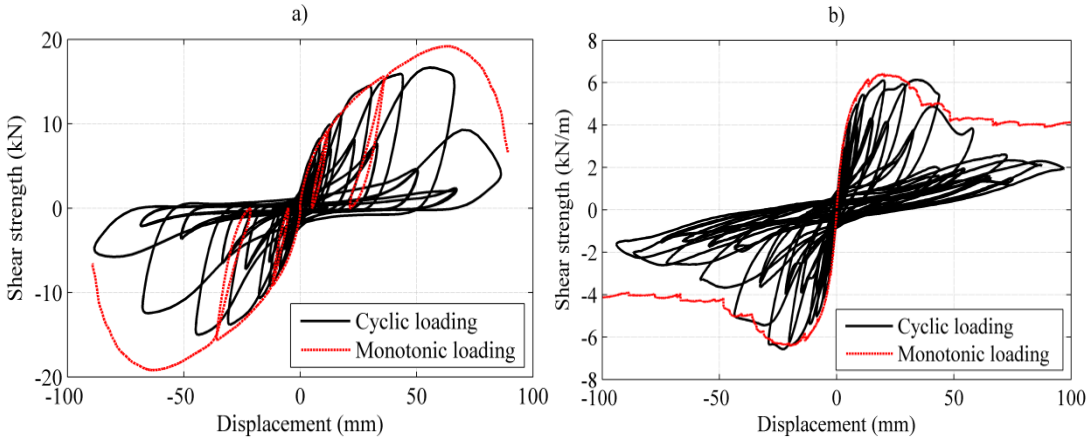

Fig.5: Comparison between monotonic and cyclic test results of wood sheathed, and steel sheathed CFS SWP.

The above described degradation modes are assumed to occur in the nonlinear domain. However, the CFS SWP could experience light degradations at low displacement amplitudes in the elastic range due to repeated cyclic displacement. The effect of low-cycle fatigue is included in CFSWSWP and CFSSSWP by using load cycle counting through the rain flow process. There is also an efficient substitute solution for this phenomenon in the OpenSees program, the Fatigue material developed by Uriz and Mahin (2008) is a wrapper function that can be used on any other material to include the effects of low cycle fatigue in its formulation.

The rates of degradation are related to the physical and mechanical characteristics of SWP as follow:

$$\delta_i^{(f/d)+} = \left(\frac{E_i}{10*E_{monotonic}}\right) \leq \delta_{limit} \; \forall \; E_i > E_{elastic} \tag{2}$$

$$\delta_i^{(f/d)-} = \left(\frac{E_i}{10*E_{monotonic}}\right) \tag{3}$$

where

$$\delta_{limit} = 0.10\left(\left(\frac{H}{2.W}\right).\left(\frac{S_c}{152}\right)\right) \tag{4}$$

$\delta_i^{(f/d)+}$ and $\delta_i^{(f/d)-}$: strength/stiffness degradation rate values for the positive and negative excursions, respectively;

δ_{limit} : maximum deterioration rate value in positive direction;

H and W : height and width of the SWP, respectively;

S_c : screw spacing at SWP perimeter;

E_i, $E_{monotonic}$, and E_e: accumulated hysteresis energy, energy required to achieve displacement at failure, and recoverable elastic strain energy, respectively.

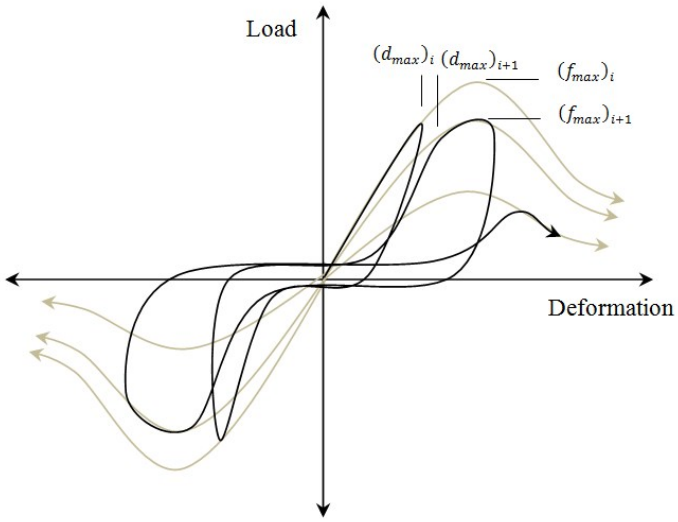

Fig.6: Impact of hysteresis damage on load-deformation response.

The stiffness degradation of the proposed model is positively related to strength degraded degree, and is defined in a same way as the strength degradation.

The stiffness and strength degradation are defined as follow:

$$f_{max,i} = f_{\max 0} \cdot \left(1 - \delta_i^f\right) \quad (5)$$

$$d_{max,i} = d_{\max 0} \cdot \left(1 + \delta_i^d\right) \quad (6)$$

Where f_{max} is the maximum strength of the response envelope, δ_i^f is the strength degradation index; d_{max} is the maximum historic displacement demand and target for reloading, δ_i^d is the reloading stiffness degradation index, and subscripts i and 0 refer, respectively, to load step i (degradation at time t) and the initial load step (where no damage has already taken place).

3. OpenSees finite element model of CFS SWP

In order to account for the overall lateral stiffness and strength of the SWP, an equivalent simple non-linear zeroLength element with CFSWSWP/CFSSSWP model connected to rigid Truss elements which transmit the force to the end elements (chord studs) that resist to uniaxial tension and compression stress (Fig.7). This modeling tip lead to a considerable reduction in terms of element number constituting the CFS SWP. The boundary members form a mechanism and lateral stiffness and strength are derived directly from zeroLength element. The CFS SWP details, as well as the schematic representation of finite element (FE) model are illustrated in Fig.7.

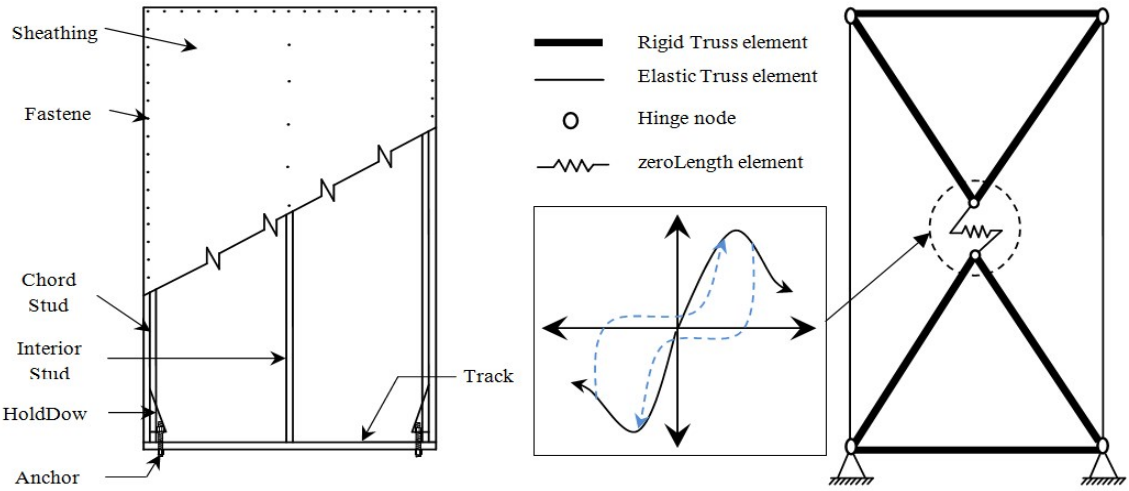

Fig.7: CFS SWP details and equivalent OpenSees FE model simple truss and zeroLength elements.

In order to check the accuracy of the proposed models, quasi-static non-linear analyses of CFS SWP have been carried out using OpenSees software. For this purpose, specimen No 26 and No 32 tested by Branston et al. (2006), and specimen 3C-a tested by Balh (2010) were selected from the literature and analyzed under similar loading conditions. This set of specimens covers a wide range of variation in physical and mechanical characteristics such as: spacing, number, shear strength, diameter of screw fasteners (s_c, n_c, V_s, and d_s); wall aspect ratio (H/W); frame thickness, chord stud moment of inertia, chord stud cross section area, interior stud moment of inertia, yield and tensile strengths of steel frame (t_f, I_{fe}, A_f, I_{fi}, F_{yf}, and F_{uf}); type of sheathing wood/steel, sheathing thickness, yield and tensile strengths of sheathing (type, t_s, F_{ys}, and F_{us}); as well as the anchor bolt diameter of the HoldDown system (d_t) are shown in Fig.8, and Fig.9.

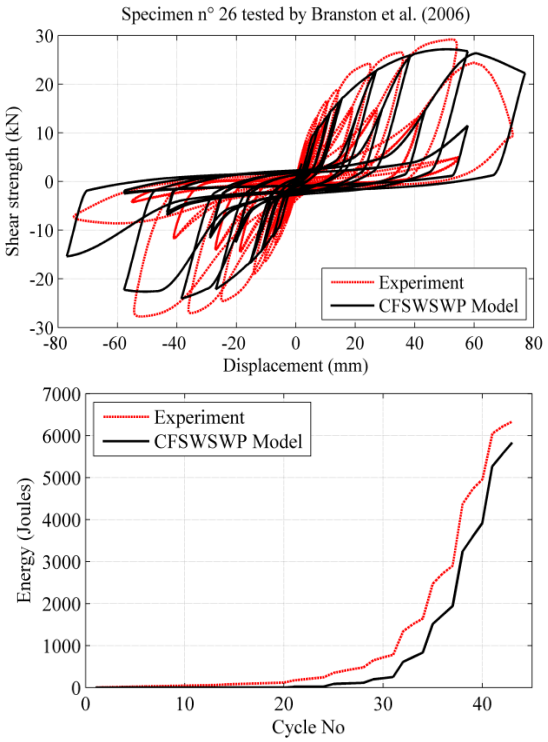

H (mm)	2440
W (mm)	1220
f_{uf} (MPa)	344
t_f (mm)	1.12
I_{fe} (mm^4)	181600
I_{fi} (mm^4)	51240
t_s (mm)	11
n_p	1
d_s (mm)	4.064
V_s(N)	3256
s_c (mm)	76
n_c	98
Type	OSB
Opening_Area (mm^2)	0
opening_Length (mm)	0

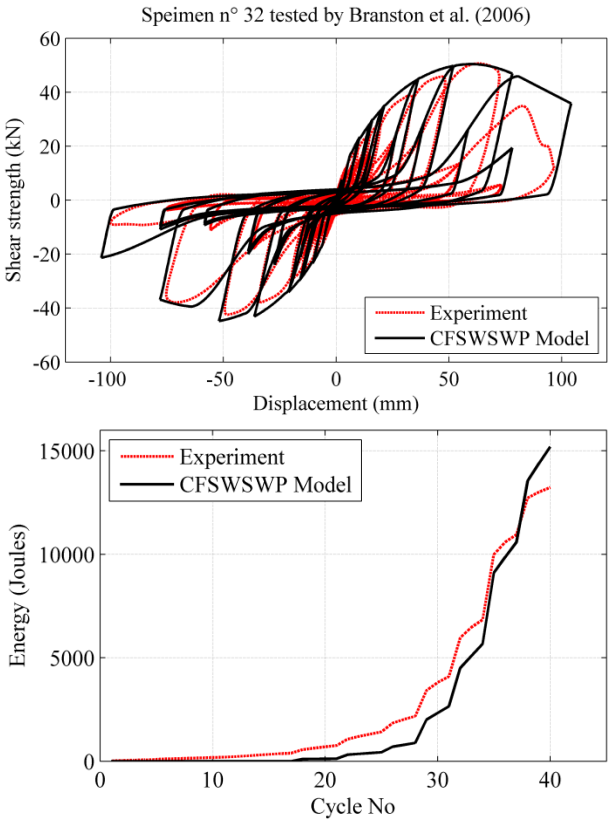

H (mm)	2440
W (mm)	2440
f_{uf} (MPa)	344
t_f (mm)	1.12
I_{fe} (mm^4)	181600
I_{fi} (mm^4)	51240
t_s (mm)	12.5
n_p	1
d_s (mm)	4.064
V_s(N)	3256
s_c (mm)	102
n_c	98
Type	CSP
Opening_Area (mm^2)	0
opening_Length (mm)	0

Fig.8: Comparison between wood sheathed CFS SWP experimental and numerical results.

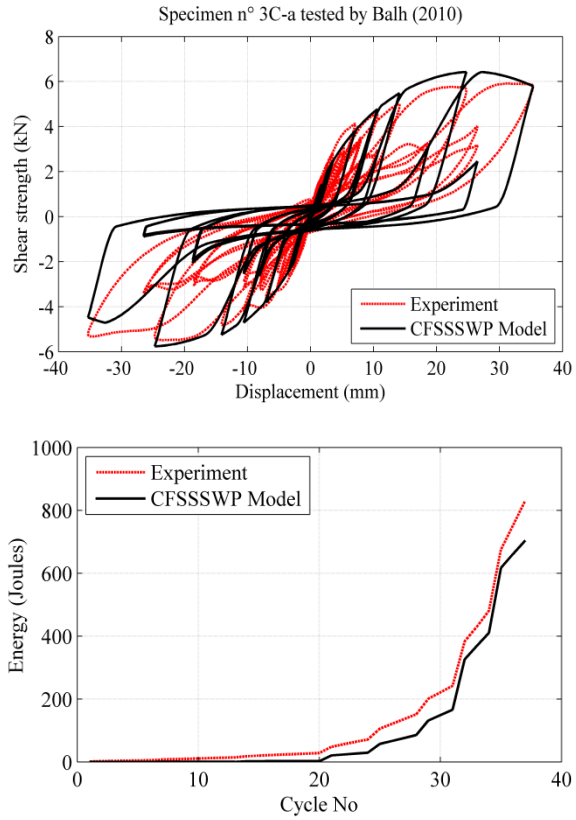

H (mm)	2440
W (mm)	1220
f_{uf} (MPa)	391
f_{yf} (MPa)	342
t_f (mm)	0.87
A_f (mm^2)	436.22
f_{us} (MPa)	395
f_{ys} (MPa)	300
t_s (mm)	0.46
n_p	1
d_s (mm)	4.166
V_s (N)	1560
s_c (mm)	150
d_t (mm)	22.2
Opening_Area (mm^2)	0
opening_Length (mm)	0

Fig.9: Comparison between steel sheathed CFS SWP experimental and numerical results.

The shear strength-lateral displacement hysteresis curves as well as the cumulative energy dissipation of wood and steel sheathed CFS SWPs from tests are plotted along with finite element results, respectively, in Fig.8, and Fig.9. In general, a good agreement is observed between the experimental and numerical results.

It is noticed from these figures that the CFSWSWP/CFSSSWP model simulates the fundamental response characteristics of the CFS SWP such as: strength and stiffness degradation, as well as the pinching effect reasonably well. The positive loops' performance of the cyclic response is better than negative ones in terms of strength capacity; this is due to the fact that the SWP is loaded first in positive direction, therefore the ability of the SWP to resist shear load in the negative side becomes weak because of the deteriorations experienced during positive incursions. This behavior is well captured using CFSWSWP and CFSSSWP models.

Discrepancies in post-peak point at which the specimens experienced a sudden decrease in shear resistance due to the detachment, at the connections, of the sheathing from CFS frame. Once the sheathing had become detached from the frame during testing, lateral stiffness and strength of the wall become substantially lower showing no clear trend due to the change in load transfer mechanism in the wall (Shamim I and Rogers CA (2013)), and hence, the proposed models are not as accurate.

APPENDIX A

CFSWSWP hysteresis model commands implemented in OpenSees

CFSWSWP hysteresis model commands for wood sheathed cold-formed steel shear wall panel

uniaxialMaterial CFSWSWP tag? height? width? f_{uf}? t_f? I_{fe}? I_{fi}? t_s? n_p? d_s? V_s? s_c? n_c? type? opening_Area? opening_Length?

tag	Integer identifier used to tag the material model
height	SWP's height (mm)
width	SWP's width (mm)
fuf	Tensile strength of framing members (MPa)
t_f	Framing thickness (mm)
Ife	Moment of inertia of the double end-stud (mm^4)
Ifi	Moment of inertia of the intermediate stud (mm^4)
t_s	Sheathing thickness (mm)
n_p	Sheathing number (one or two sides sheathed)
d_s	Screws diameter (mm)
V_s	Screws shear strength (N)
s_c	Screw spacing on the sheathing perimeter (mm)
n_c	Total number of screw on the sheathing
type	Integer identifier used to define wood sheathing type (DFP=1, OSB=2, CSP=3)
opening_Area	Totale area of openings (mm^2)
opening_Length	Cumultive length of openings (mm)

CFSSSWP hysteresis model commands for steel sheets sheathed cold-formed steel shear wall panel

uniaxialMaterial CFSSSWP tag? height? width? f_{uf}? f_{yf}? t_f? A_f? f_{us}? f_{ys}? t_s? n_p? d_s? V_s? s_c? d_t? opening_Area? opening_Length?

tag	Integer identifier used to tag the material model
height	SWP's height (mm)
width	SWP's width (mm)
fuf	Tensile strength of framing members (MPa)
fyf	Yield strength of framing members (MPa)
t_f	Framing thickness (mm)
A_f	Framing cross section area (mm²)
fus	Tensile strength of steel sheet sheathing (MPa)
fys	Yield strength of steel sheet sheathing (MPa)
t_s	Sheathing thickness (mm)
n_p	Sheathing number (one or two sides sheathed)
d_s	Screws diameter (mm)
V_s	Screws shear strength (N)
s_c	Screw spacing on the sheathing perimeter (mm)
d_t	Anchor bolt's diameter (mm)
opening_Area	Totale area of openings (mm²)
opening_Length	Cumultive length of openings (mm)

APPENDIX B

1. Chart of iterative procedure for each lateral shear displacement

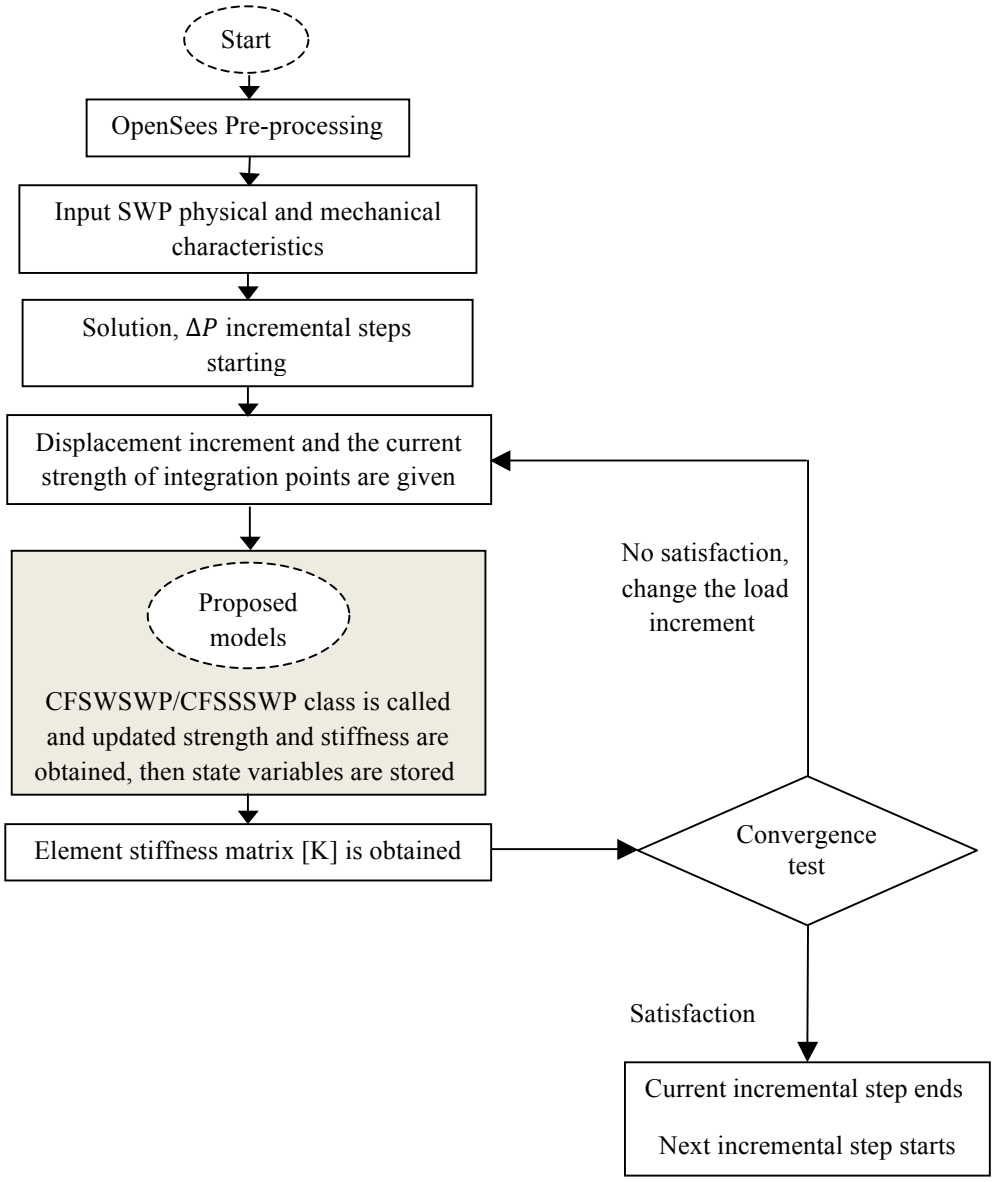

2. Strength and stiffness determination chart of steel and wood sheathed CFS SWP.

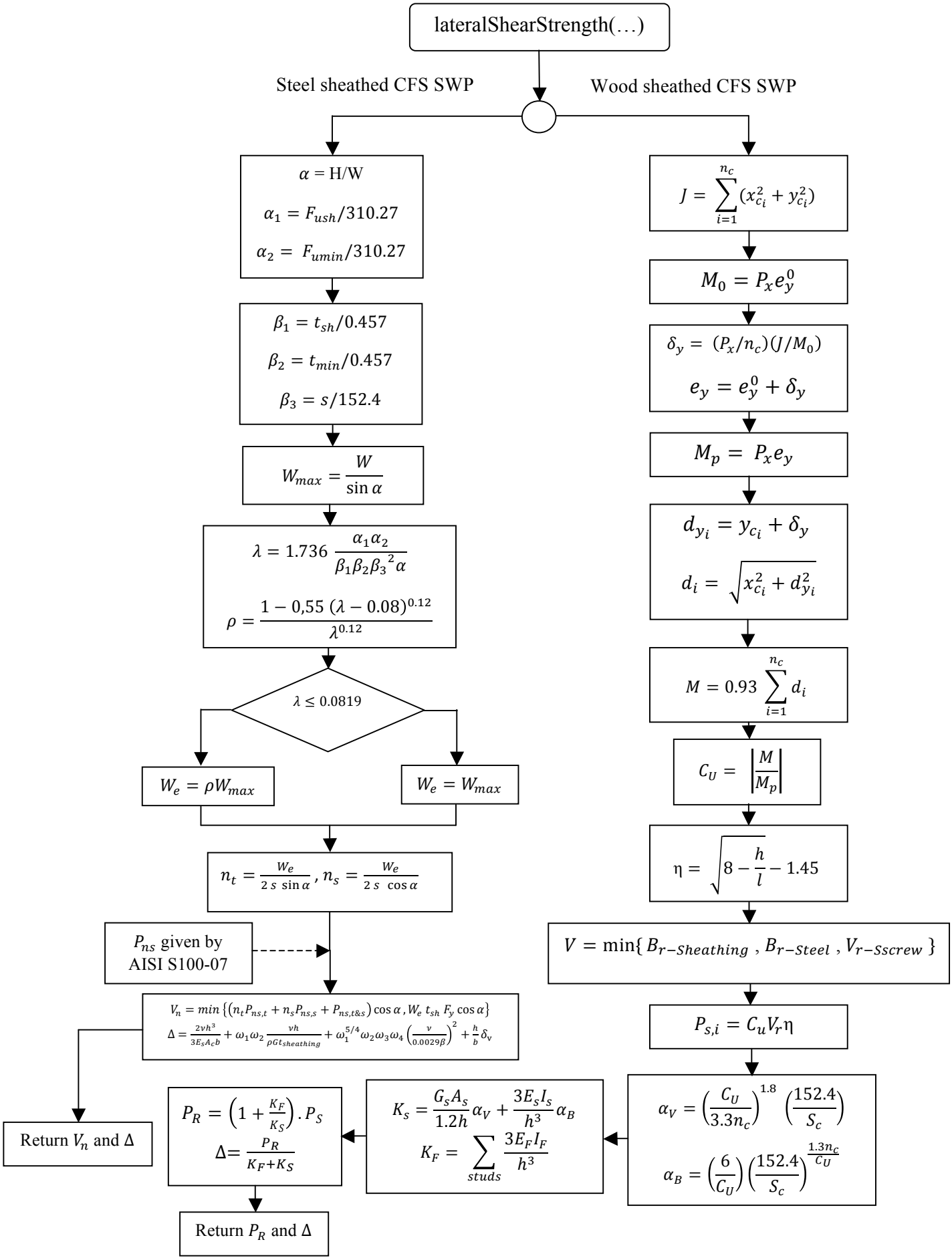

APPENDIX C

Numerical models and corresponding quasi-static tests' results

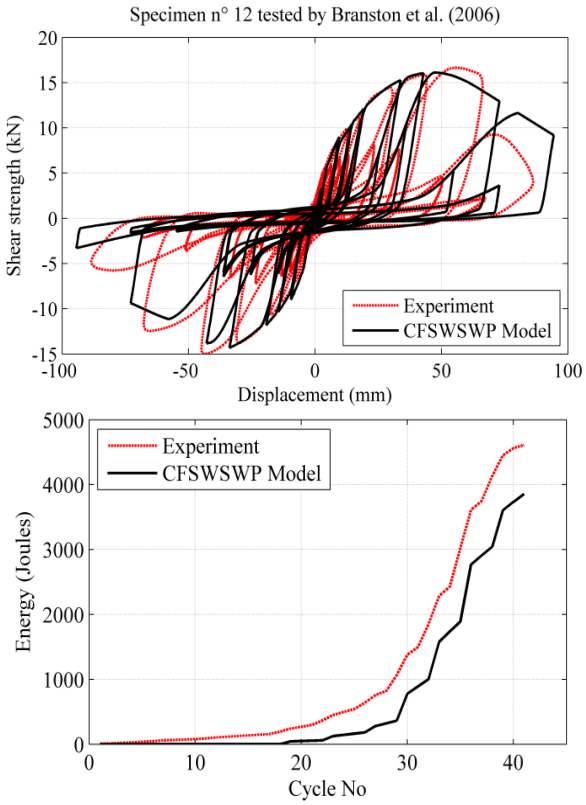

H (mm)	2440
W (mm)	1220
f_{uf} (MPa)	344
t_f (mm)	1.12
I_{fe} (mm^4)	181600
I_{fi} (mm^4)	51240
t_s (mm)	12.5
n_p	1
d_s (mm)	4.064
V_s (N)	3256
s_c (mm)	152
n_c	50
type	DFP
Opening_Area (mm^2)	0
Opening_Length (mm)	0

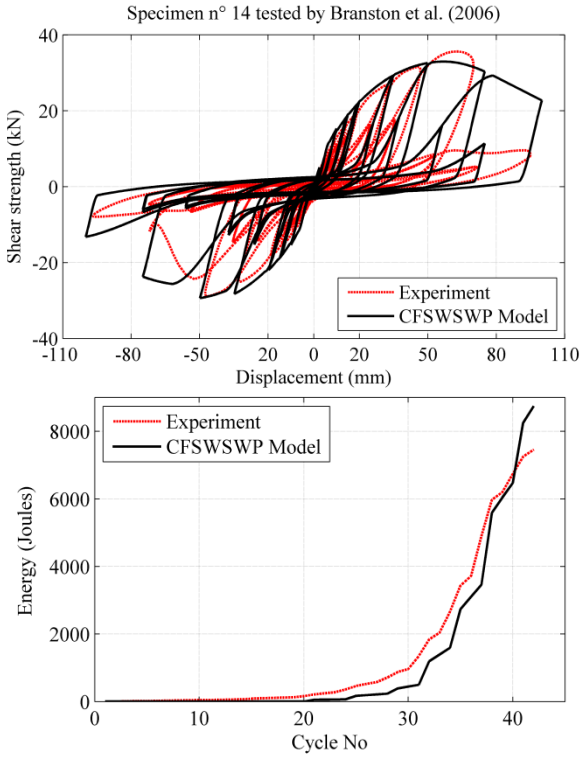

H (mm)	2440
W (mm)	1220
f_{uf} (MPa)	344
t_f (mm)	1.12
I_{fe} (mm^4)	181600
I_{fi} (mm^4)	51240
t_s (mm)	12.5
n_p	1
d_s (mm)	4.064
V_s (N)	3256
s_c (mm)	76
n_c	98
Type	DFP
Opening_Area (mm^2)	0
Opening_Length (mm)	0

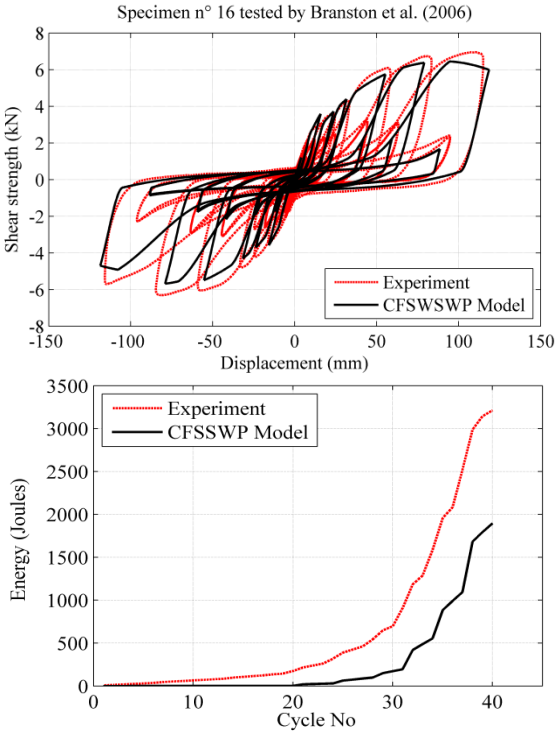

H (mm)	2440
W (mm)	610
f_{uf} (MPa)	344
t_f (mm)	1.12
I_{fe} (mm^4)	181600
I_{fi} (mm^4)	51240
t_s (mm)	12.5
n_p	1
d_s (mm)	4.064
V_s (N)	3256
s_c (mm)	152
n_c	40
type	CSP
Opening_Area (mm^2)	0
opening_Length (mm)	0

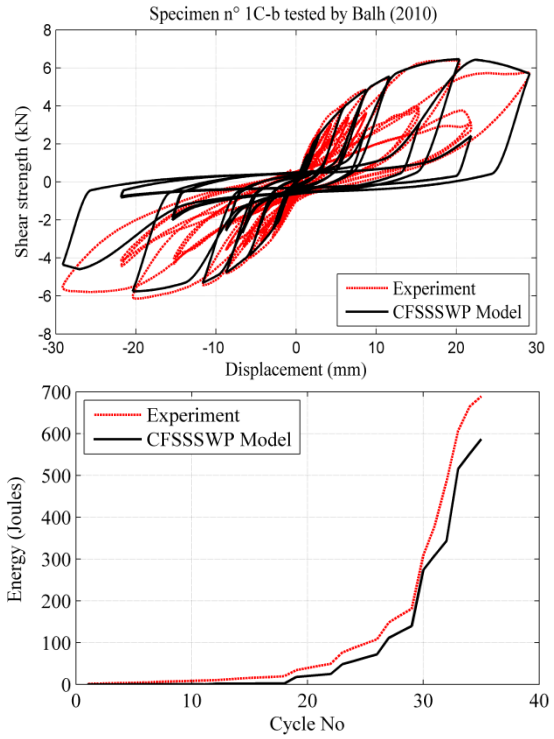

H (mm)	2440
W (mm)	1220
f_{uf} (MPa)	496
f_{yf} (MPa)	346
t_f (mm)	1.14
A_f (mm^2)	436.22
f_{us} (MPa)	395
f_{ys} (MPa)	300
t_s (mm)	0.46
n_p	1
d_s (mm)	4,166
V_s (N)	1560
s_c (mm)	150
d_t (mm)	22.2
Opening_Area (mm^2)	0
opening_Length (mm)	0

References

Balh N (2010) "Development of seismic design provisions for steel sheathed shear walls", Master Thesis, McGill University, Canada.

Bourahla N, Berdiafe-Bourahla M, El djouzi B, Meddah H, Allal N (2012) "Post Elastic Modelling Techniques and Performance Analysis of Cold Formed Steel Structures Subjected to Earthquake Loadings", 15th World Conference on Earthquake Engineering, Lisbon, Portugal, 24-28 September.

Branston AE, Chen CY, Boudreault FA, Rogers CA (2006) "Testing of light-gauge steel frame wood structural panel shear walls", Canadian Journal of Civil Engineering 2006; 33(5):573–87.

DaBreo J (2012) "Impact of Gravity Loads on the Lateral Performance of Cold-Formed Steel Frame/Steel Sheathed Shear Walls", Master Thesis, McGill University, Canada.

Kechidi S (2014) Hysteresis model development for cold-formed steel shear wall panel based on physical and mechanical characteristics, Master Thesis, University of Blida 1, Algeria

Liu P, Peterman K.D, Yu C, Schafer B.W (2012) "Characterization of cold-formed steel shear wall behaviour under cyclic loading for CFS-NEES building", Proceedings of the 21st International Specialty Conference on Cold-Formed Steel Structures, St. Louis, MO.

Lowes LN and Altoontash A (2003) "Modelling Reinforced-Concrete Beam-Column Joints Subjected to Cyclic Loading", Journal of Structural Engineering, 129:1686-1697.

Mazzoni S, McKenna F, Scott MH, Fenves GL (2009) Open system for earthquake engineering simulation; user command language manual, University of California at Berkeley, USA

Serrette R, David P, Nolan PE (2009) "Reversed Cyclic Performance of Shear Walls with Wood Panels Attached to Cold-Formed Steel with Pins", Journal of Structural Engineering, 135:959-967.

Shamim I and Rogers CA (2013) "Steel sheathed/CFS framed shear walls under dynamic loading: Numerical Modelling and Calibration", Thin-Walled Structures, 71:57–71.

Uriz P, Mahin S. Toward earthquake-resistant design of concentrically braced steel-frame structures. PEER report. University of California, Berkeley, 2008.

Xu L and Martinez J (2006) "Strength and Stiffness Determination of Shear Wall Panels in Cold-Formed Steel Framing", Thin-Walled Structures, 44(12):1084-1095.

Yanagi N, Yu C (2014) "Effective strip method for the design of cold-formed steel framed shear wall with steel sheet sheathing", Journal of Structural Engineering, ASCE 2014; 140(4).